

Cite this: DOI:[10.56748/ejse.25713](https://doi.org/10.56748/ejse.25713)Received Date: 23 November 2024
Accepted Date: 2 May 2025

1443-9255

<https://ejsei.com/ejse>Copyright: © The Author(s).
Published by Electronic Journals
for Science and Engineering
International (EJSEI).This is an open access article
under the CC BY license.<https://creativecommons.org/licenses/by/4.0/>

Predictive Modeling of Compressive Strength and Slump in High-Performance Concrete Utilizing Machine Learning

Yu Yang ^a, Ye Chen ^a, Peng Zhang ^b, Weining Zhang ^{a*},^a Department of Architecture, Shijiazhuang Institute of Railway Technology, Shijiazhuang 050000, Hebei, China^b Maintenance Department, Shang'an Huaneng Power International, INC., Shijiazhuang 050000, Hebei, China*Corresponding author: 18822585853@163.com

Abstract

Compressive strength (CS) is a crucial property of high-performance concrete (HPC) as it determines its ability to withstand applied stress without breaking or deteriorating. It ensures structural stability and durability and, hence, resistance to various types of external loads, which is critical for infrastructure serviceability over a long period of time. Whereas slump (SL) is indicative of the uniformity and workability of HPC, it affects the ease of placing and consolidation, as well as construction quality and efficiency. Mix design optimization, through proper balancing between CS and SL, enhances the capability of HPC to meet the stringent operational standard for heavy applications like bridges, high-rise buildings, and nuclear facilities concerning safety and longevity with cost-effectiveness while constructing the projects. The research estimated the CS and SL of the HPC by advanced machine learning (ML) regression frameworks such as Adaptive boosting regression (ADAR), Support vector regression (SVR), and two optimizers: Giant Armadillo Optimization Framework (GOA) and Chef Based Optimization Framework (CBOA). Combining these frameworks with an optimizer result in a novel hybrid framework that offers enhanced precision and functionality. Results show that the ADA+GOA (ADGA) model performs the best in predicting CS, achieving an RMSE of 2.451 and an R^2 value of 0.992. In comparison, the ADA+CBOA (ADCB) model also outperforms the base ADA model, with an RMSE of 3.618 and an R^2 value of 0.982. Notably, the SVR and its hybrid variants exhibit poorer performance, with higher RMSE and lower R^2 values compared to the ADA-based models. These results then emphasize the capability of hybrid ML frameworks to predict the characteristics of concrete with a good degree of accuracy.

Keywords

High-performance concrete, Slump, Compressive strength, Machine learning (ML), Metaheuristic frameworks

1. Introduction

Compressive strength (CS) is one of the most important mechanical parameters characterizing the material capability to bear axial compressive stresses without breakdown (Vu et al., 2020). CS plays a very significant role in the design and analysis of elements of construction in different branches of engineering sciences, namely civil, mechanical, and engineering (Moccia et al., 2021; Tasevski et al., 2019). The value of CS is usually determined following standardized test procedures specific to particular industries or regulatory requirements (Liu and Li, 2019). Logically, it defines CS as the maximum stress a material can bear without failure (Paudel et al., 2023). It is quantified in terms of pressure per unit area, such as MPa or pounds per square inch (Khajavi et al., 2025; Sadaghat et al., 2024), and for concrete—arguably one of the most common substances whose is tested the CS usually expressed as f_c (Napoli and Realfonzo, 2020; Tavana Amlashi et al., 2023). A number of factors contribute to CS for a material, namely, permeability, moisture, aggregate distribution, and microstructure (Murali et al., 2023). Within concrete, for instance, CS is a function of the water-to-cement ratio, type and size of aggregate, conditions of curing, and admixtures present (Malhotra, 1956; Naeim et al., 2024b). CS consideration might be crucial for materials with respect to the structural design and analysis. This functionality allows designers to analyze the strength and durability of structures such as dams, bridges, buildings, and highways (Ni and Wang, 2000). If the CS of building materials is kept at, or above, design specifications, then engineers are able to reduce the risk of structural failure and promote a longer service life for structure and infrastructure (Kim and Yi, 2002).

Several influential factors affect CS, one of the fundamental properties of concrete. First, the water-cement ratio is quite critical; the intensity is usually greater when the ratio is lower due to reduced porosity and better hydration of the cement (Salem and Pandey, 2015). Second is the aggregate-cement ratio; the strength is affected by a well-graded aggregate mix since improvements in packing and interlocking result in improved strengths (Abdullahi, 2012). Third, the quality of the ingredients themselves is one of the influencing factors on strength: cement, aggregate, and water might contain contaminants or have poor grading that can result in matrix weakness (Aginam et al., 2013a; Ngugi et al., 2014; Obi Lawrence, 2016). Fourth, curing conditions come into play: under the most favorable conditions of moisture and temperature, normal hydration is usually fully developed (Atiş et al., 2005). Fifth, another critical factor

involves age; strength normally gains with time as a result of hydration; the rate, however, depends on curing circumstances (Pourbaba et al., 2018). The presence of admixtures can alter hydration kinetics or increase workability and affect the strength of concrete (Sharma, 2021). The seventh is the surrounding conditions, temperature, and humidity during curing and service life that determine the characteristics of strength growth and durability (Ambroziak and Ziolkowski, 2020). Lastly, the overall mix design, with its additives and proportions in concrete, governs the overall performance. It is well recognized that the understanding and control of these parameters have a close bearing on achieving optimum CS in concrete applications (Aginam et al., 2013b).

The slump (SL) of high-performance concrete (HPC) is a measure of consistency or workability, which is relevant to most building applications (Yen et al., 1999). It is done by investigating the settlement or deformation of a cone of fresh concrete subjected to a given amount of compacting (Chen et al., 2014). The SL test, according to recognized standards such as ASTM C143 or EN 12350-2, is done by filling fresh concrete into a metal cone, compacting it by vibration in layers, and then removing the cone and measuring the subsidence of the concrete mass vertically (Mahajan et al., 2020; Tan et al., 2017). With improved aggregate distribution and enhanced material properties, HPC also exhibits favorable slump characteristics. The type and proportion of cementitious materials, water-cement ratio, chemical admixtures, aggregate gradation, and supplemental cementitious materials are some factors that would affect an SL (Naeim et al., 2024a). These together constitute the rheological behavior of the concrete mixture, hence its flowability, viscosity, and form-sustaining ability. In the passive voice, many factors affect the SL of the HPC (Islam et al., 2012). The water/cement ratio is correctly controlled to provide the appropriate slump while sustaining strength and durability (Zhutovsky and Kovler, 2017). In this respect, chemical admixtures, including superplasticizers, are habitually used to improve workability and to prevent SL loss throughout the life of concrete, for instance, (Dushimimana et al., 2021; Farzadnia et al., 2011).

Accordingly, supplementary cementitious materials such as fly ash or silica fume could modify the rheological properties of concrete mix and thereby influence SL behavior (Mosaberpanah and Umar, 2020). Well-graded aggregates, with proper particle size distribution, tend to have internal cohesion and reduce segregation; hence, it may affect SL variability (Hasan et al., 2022). Understanding the SL characteristics of HPC is of paramount importance for proper consolidation, placement, and finishing during construction (Parande, 2013). Correct SL values are

necessary for engineers and contractors to modify mixed designs and construction methodologies to meet project specifications and operational expectations. SL control in HPC improves construction efficiency and the long-term operation and reliability of infrastructure (Jonnalagadda and Chava, 2023).

1.1 Related Works

Recently, according to Ahmad, Aynaz, and Furqan et al. (A. Ahmad et al., 2021a, 2021b, 2021c; Algaifi et al., 2021; Amin et al., 2021; Ruggieri et al., 2021; Shah et al., 2022), ML frameworks have shown a significant ability in predicting cement-based material properties. Support vector regression (SVR) and Artificial neural network (ANN) are some of the common machine learning (ML) methods that Alexandridis et al. (Alexandridis et al., 2015) successfully used to predict the properties of concrete such as CS, split-tensile strength, elastic modulus, and so on (Chaabene et al., 2020; DeRousseau et al., 2018; Song et al., 2021a). Thus, they are considered individual frameworks. Many fields of study have, in fact, shown that through the integration of results from a discrete framework into an ensemble ML model pattern, the accuracy of predictions can be considerably better (Chaabene et al., 2020). However, few workers in this area have used EML to predict factors. AdaBoost and Random Forest (RF) are learning methods that can improve accuracy prediction based on numerous regression tree forecasts combined through voting on the conclusion (Sun et al., 2021). Ahmad et al. (W. Ahmad et al., 2021) adopted solo and EML methods in estimating the CS of concrete and comparing their precision. EML methods were proven to forecast the outcomes with superior accuracy compared to solo methodologies. However, the independent process also yielded acceptable results. Song et al. (Song et al., 2021b) performed an experimental study to predict, by independent techniques, the C-S of concrete containing ceramic waste. It was observed from the study that the output from the prediction model matched the experimental results. Abuodeh et al. (Abuodeh et al., 2020) predicted, by using the ANN technique, the C-S for ultra HPC and stated that ANN worked adequately in the prediction of results. Consequently, the current research focuses on the use of advanced techniques in predicting the properties of concrete. Extensive research on HPC's mechanical properties often involves time-consuming lab procedures. To address this, ML approaches were explored for predicting 28-day CS.

1.2 Innovations

The paper has introduced a hybrid machine learning model incorporating ADAR and SVR with new metaheuristic optimizers, including the Giant Armadillo Optimization Framework (GOA) and the Chef-Based Optimization Framework (CBOA). Needless to say, the new hybrid models that are proposed have outperformed conventional methods in stand-alone with respect to better prediction precision and functionality. It presents a comparative performance evaluation of such frameworks using comprehensive performance metrics, including RMSE (Root Mean Square Error), R^2 (Coefficient of Determination), MAE (Mean Absolute Error), SI (Scatter Index), and MNB (Mean Normalized Bias), for bringing out the effectiveness of such framework's ineffective prediction of major concrete properties like CS and SL. Among those, some of the novelties of this research are the huge dataset analyzed to influence the effect of critical factors such as the water binder ratio, fly ash, water, silica fume, superplasticizer dosage on the properties of HPC. This degree of precision would suggest that predictive modeling could serve to raise mixed design performance regarding operational efficiency and material optimization.

2. Datasets and ML Frameworks

2.1 Description of the Dataset

In this study, water binder ratio, fly ash, water, silica fume, and superplasticizer are of considerable importance in affecting the CS and SL of the HPC, based on the objective. A relationship between each of these properties and anticipation using ML in CS and SL will be explored.

- **Water Binder Ratio:** The water/binder ratio is one of the most critical parameters in the mix design of concrete, as it influences both CS and SL. ML frameworks consider how different water/binder ratios affect these properties by training models with datasets of ratios versus the corresponding CS and SL values for proper predictions of property change.
- **Fly Ash:** Fly ash is one of the ordinary pozzolanic materials widely used in HPC for supplementary cementitious components. ML frameworks analyze the CS and SL value datasets regarding the proportion for estimating the optimum content of fly ash that may provide the desired properties in concrete.
- **Water:** Added water highly affects CS and SL in concrete. After training on datasets for the water-cement ratio and the respective concrete

properties, the ML framework can predict how much water would yield target characteristics in concrete.

- **Silica Fume:** Silica fume is an amorphous SF supplementary cementitious material that greatly improves the strength and durability of concrete. The ML framework can peruse a dataset of SF concentration with CS and SL values to estimate the optimum dosage for different concrete performances.
- **Superplasticizer:** Superplasticizers enhance concrete workability without adding water. ML frameworks, trained in datasets of superplasticizer dosages and their effects on CS and SL, can predict the optimal dose to achieve desired concrete properties.

Basically, ML can delve deep into the inter-relationships among water binder ratio, fly ash, water, silica fume, and superplasticizer content and their varying effects on CS and SL in HPC. With the help of ML frameworks, investigators are able to reach the optimal concrete mix designs that could meet the specified operation standards from various construction applications. Next, the varying influences exerted by different factors on CS and SL are elaborated in detail with the help of Table 1 and Fig. 1.

Table 1. The statistical properties of the input factor of CS-SL.

Factors	Indicators				
	Category	Min	Max	Avg	St.Dev.
W/B (%)	Input	18.000	45.000	31.095	8.701
W (kg/m ³)	Input	140.000	180.000	162.143	12.009
s/a (%)	Input	35.000	53.000	42.143	5.323
FA (%)	Input	0.000	20.000	5.714	7.911
AE (kg/m ³)	Input	0.000	0.078	0.031	0.029
SF (%)	Input	0.000	25.000	6.429	8.330
SP (kg/m ³)	Input	1.890	36.500	10.956	8.513
CS (MPa)	Output	38.000	123.000	74.402	26.437
Slump(mm)	Output	95.000	260.000	203.132	25.645

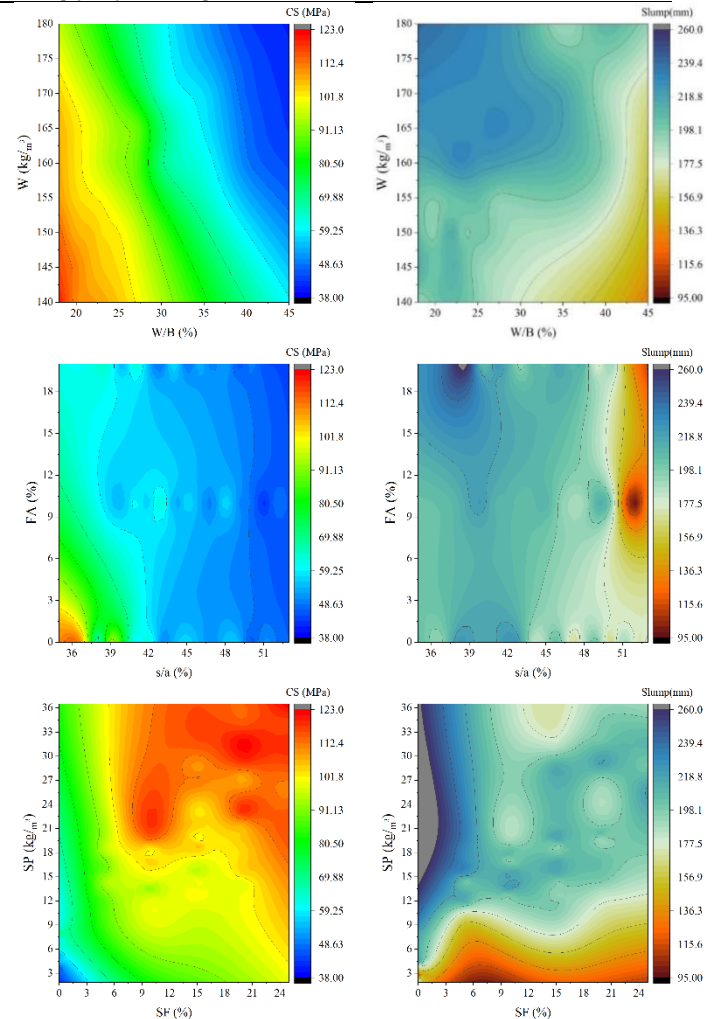


Fig. 1 The contour plot for the relation between the input and output variables.

Fig. 1 presents contour plots illustrating the relationships between input and output variables in HPC mix design. Each plot analyzes three variables: two input parameters (X and Y) and one output variable (Z), representing either CS or SL. The selection of relationships, W with W/B, FA with s/a, and SP with SF, was based on their critical role in determining HPC properties. W and the W/B significantly influence both workability and strength, making their relationship essential for optimizing HPC

performance. Similarly, FA and the s/a affect the mixture's cohesiveness, particle packing, and overall durability. The interaction between SP and SF is also crucial, as these admixtures improve the rheological properties and mechanical performance of HPC. These contour plots provide a visual representation of how variations in input parameters impact the key performance metrics of HPC, aiding in the optimization of mix design.

2.2 Operation Evaluator

The performance of the proposed models was evaluated using multiple statistical metrics to ensure accuracy and reliability. Root Mean Square Error (RMSE) measures the average deviation between predicted and actual values, with lower values indicating better performance. The Coefficient of Determination (R^2) assesses how well the model explains variance in the data, where values closer to 1 signify stronger predictive capability. Mean Absolute Error (MAE) quantifies the average magnitude of errors, providing a straightforward measure of prediction accuracy. The Symmetric Mean Absolute Percentage Error (SI) ensures a scale-independent evaluation of errors, making it useful for comparative analysis. Lastly, the Mean Normalized Bias (MNB) identifies systematic over- or under-prediction tendencies, offering insights into model bias. The equation of the evaluation metrics is as follows:

$$RMSE = \sqrt{\frac{1}{n} \sum_{i=1}^n (y_i - \hat{y}_i)^2} \quad (1)$$

$$R^2 = 1 - \frac{\sum_{i=1}^n (y_i - \hat{y}_i)^2}{\sum_{i=1}^n (y_i - \bar{y})^2} \quad (2)$$

$$MAE = \frac{1}{n} \sum_{i=1}^n |y_i - \hat{y}_i| \quad (3)$$

$$SI = \frac{1}{n} \sum_{i=1}^n \frac{|y_i - \hat{y}_i|}{(|y_i| + |\hat{y}_i|)/2} \quad (4)$$

$$MNB = \frac{1}{n} \sum_{i=1}^n \frac{y_i - \hat{y}_i}{y_i} \quad (5)$$

Here y_i shows the measured value, \hat{y}_i shows the predicted value, \bar{y} shows the mean value of the predicted value, and n is the number of samples.

3. Results and Discussion

The results and discussion section comprehensively evaluates the ML models' performance in predicting HPC properties. The analyses were conducted by training the models on the dataset optimizing hyperparameters to maximize prediction accuracy. The models were then tested using a separate dataset to evaluate generalization capability. Performance was assessed using several statistical metrics, including RMSE, R^2 , MAE, SI, and MNB, which provide insights into the model's accuracy, bias, and error distribution. The results were compared between base models and their hybrid counterparts, highlighting the impact of optimization algorithms on predictive performance. Additionally, sensitivity analysis was conducted to determine the most influential input parameters affecting CS and SL. The discussion interprets these findings in the context of practical applications, emphasizing the importance of optimizing HPC mix designs for enhanced structural performance and longevity.

3.1 Convergence Curve

Convergence curves are graphical representations of the iterative optimization processes of frameworks. The convergence curve represents the error reduction trends across the subsequent cycles by plotting an operation indicator representative, including error-against-cycle number or computing effort. A convergence curve showing a monotonous decrease in error indicates that the model is progressively closer to an ideal solution. On the other hand, the plateau and fluctuating curves may signify some issues with model convergence or poorly adjusted parameters. The investigation of the convergence curve enables researchers to gauge the convergence rate-ultimately the stability and anticipation precision of frameworks, thus enabling more appropriate decisions along the steps of model selection and refinement.

The following convergence curve in Fig. 2 compares the RMSE rates of SVCB, SVGA, ADCB, and ADGA frameworks under CS and SL targets. Comparing the results from these frameworks under the CS target, it is seen that the lowest error is contributed by the ADGA model with an RMSE value of 2, which starts the cycle process with an error value greater than 6. Subsequently, the ADCB model, with an RMSE value of 2.5 at cycle 80, demonstrates its potential as the second-best model, at least within this context. Conversely, the SVGA and SVCB frameworks, with RMSE values of 4 and 6, respectively, indicate weaker functionality compared to the frameworks mentioned earlier.

Under the SL target, the SVCB model, with an RMSE value of almost 8 at cycle 60, demonstrates weaker functionality compared to the SVGA model, which exhibits an RMSE value of nearly 6, and the ADCB model, with an RMSE value of practically 5 at cycle 80. Considering these observations, akin to the CS target, it is anticipated that the ADGA model, with an RMSE value of 4, showcases superior functionality compared to

the previously mentioned frameworks in this comparison (Trojovská and Dehghani, 2022).

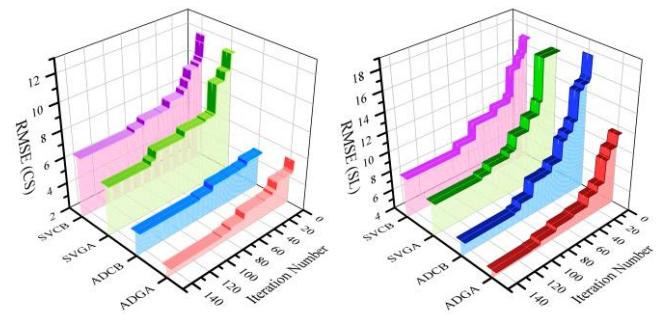


Fig. 2 The convergence curve for the presented hybrid frameworks

3.2 Frameworks Comparison

The outcomes of the utilized frameworks in the Training, Testing, and Validation steps are compared in Table 2 under CS and SL targets. In the evaluation between the ADA model and its hybrid counterparts, the ADGA model emerges as the top performer during the training step, boasting an RMSE value of 2.451. Subsequently, the ADCB model displays superior operation with a reduced error, recording an RMSE value of 3.618 compared to the ADA model's RMSE value of 4.451, particularly under the CS target. Transitioning to the SL target, within the realm of SVR and its hybrid variations, the base SVR model exhibits the highest error with an RMSE value of 4.451 during the training step. Surpassing this, the SVCB model showcases a notable decrease in error, registering an RMSE value of 3.618, indicative of enhanced operation relative to the base model. However, the SVGA model outshines both the base SVR and SVCB models, manifesting the lowest RMSE value of 2.451, thereby establishing its superiority in error mitigation. This comparative analysis demonstrates the effectiveness of hybrid frameworks in optimizing anticipated precision under a variety of scenarios (Silveira et al., 2009).

In the assessment of the CS and SL MPa of the ADA model and its hybrid forms across different targets and steps, notable distinctions emerge in Fig. 4. Under the CS target, during the validation step, the ADGA model outperforms the ADCB model due to its outcome closely aligning with the measured value, indicating superior precision and predictive capability. Conversely, under the SL target in the testing step, a comparative analysis between the ADCB and ADA frameworks reveals contrasting operations. Here, the ADA model exhibits inferior functionality compared to the ADCB model, primarily evidenced by its higher precision. In contrast, the precision value of the ADCB model demonstrates a closer approximation to the measured value, signifying its enhanced predictive precision and reliability in SL targets. In general, the data highlights the complex operation differences between the ADA model and its hybrid equivalents, underscoring the need to take into account both target-specific and step-specific parameters when evaluating predictive effectiveness.

In Fig. 5, the subsequent plot provides an overview of the frequency and error values of the employed frameworks across SL and CS targets. For instance, in the CS target, a comparison between the ADGA and ADCB frameworks demonstrates that the frequency of ADGA frameworks during the training step is approximately 35, accompanied by an error close to zero. Conversely, the frequency of ADCB frameworks hovers around 30, exhibiting a higher spread error compared to the ADGA model. Shifting focus to the SL target, a comparative analysis between the ADGA and ADCB frameworks highlights the operation disparity. The ADGA model, with a frequency of 65 and an error percentage close to zero, emerges as the more functional option. In contrast, the ADCB model registers a frequency of 48, coupled with an error percentage that deviates further from zero compared to the ADGA model. This underscores the superior efficacy of the ADGA model in minimizing errors and achieving higher frequency counts within the SL target.

In Fig. 6, the error density of the presented frameworks in the various steps is depicted along the median line, representing zero error. For instance, during the training step of the CS target, the error density of ADGA is superior to that of ADCB. Additionally, it is noted that the error density of ADA is wider than that of ADCB and ADGA. In the SL target, during the training step, the error density of the ADA model is observed to deviate notably from zero or the median line. Conversely, the operation of the ADCB model surpasses that of the base model, with its error density nearly approaching the median line, albeit not as close as the ADGA model. Notably, the ADGA model exhibits the highest error density on the median line, indicating a more centralized distribution of errors on 0.

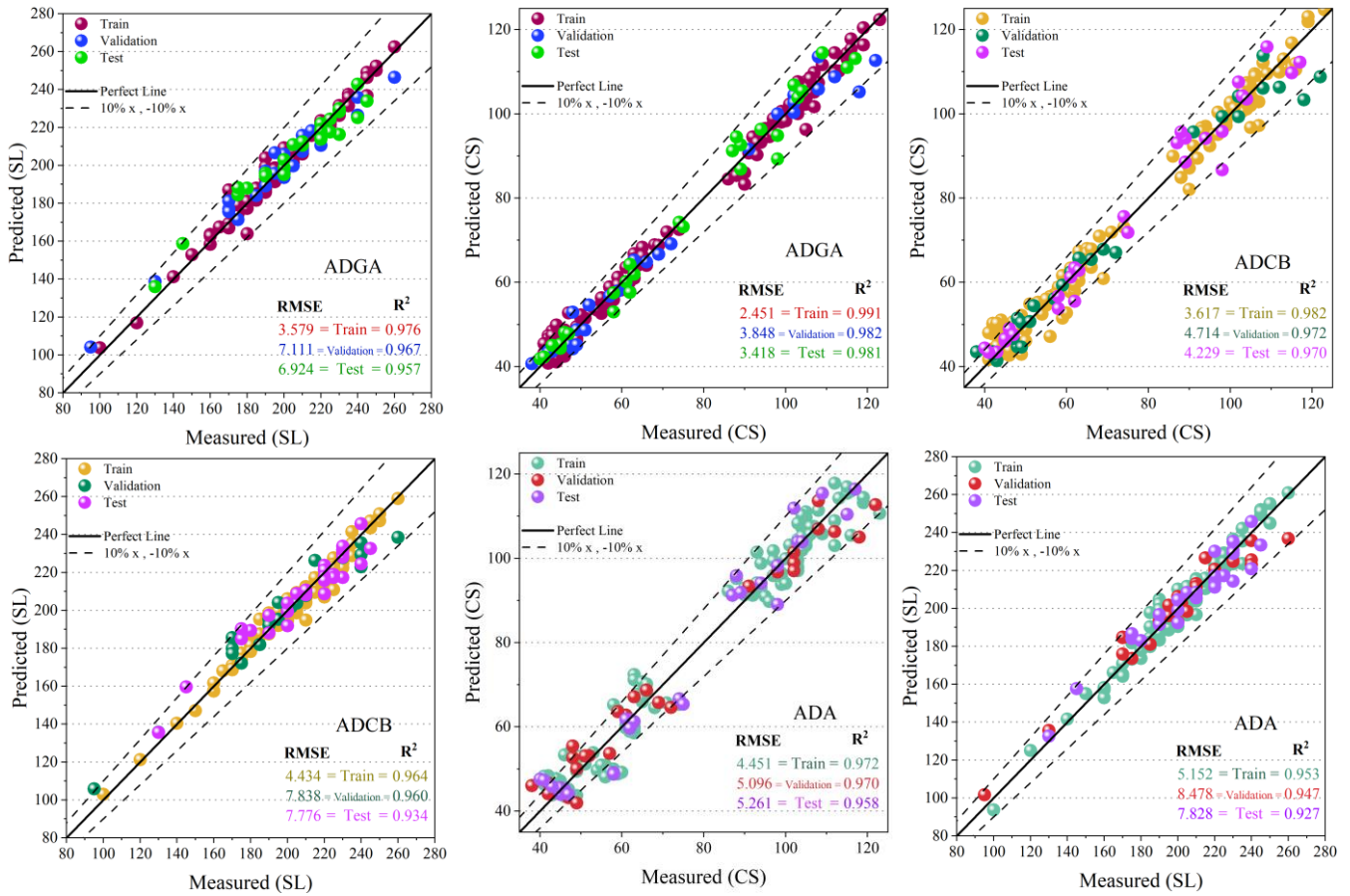


Fig. 3 The dispersion of the presented models based on CS and SL

Table 2. The result of developed models for CS and SL

Model	Step	Index values					
		RMSE	R ²	MAE	SI	MNB	
CS	ADGA	Train	2.451	0.992	1.943	0.033	-0.005
		Validation	3.849	0.982	2.764	0.053	0.006
		Test	3.418	0.981	2.733	0.045	-0.003
	ADCB	Train	3.618	0.982	2.903	0.048	-0.013
		Validation	4.714	0.972	3.271	0.065	0.002
		Test	4.229	0.971	3.193	0.056	-0.008
	ADA	Train	4.451	0.972	3.584	0.060	-0.008
		Validation	5.097	0.970	4.198	0.071	-0.009
		Test	5.262	0.958	4.002	0.070	0.002
SVGA	Train	5.717	0.957	4.914	0.077	-0.001	
	Validation	6.039	0.956	4.962	0.084	-0.019	
	Test	6.661	0.935	5.807	0.088	-0.041	
SVCB	Train	6.443	0.948	5.580	0.086	-0.011	
	Validation	7.447	0.943	6.586	0.103	-0.043	
	Test	6.964	0.931	6.329	0.092	-0.048	
SVR	Train	7.441	0.932	6.521	0.100	0.013	
	Validation	7.775	0.928	6.417	0.108	0.037	
	Test	7.639	0.912	6.544	0.101	0.014	
SL	ADGA	Train	3.580	0.976	2.524	0.018	0.000
		Validation	7.111	0.968	5.728	0.036	-0.005
		Test	6.925	0.958	5.278	0.033	-0.005
	ADCB	Train	4.434	0.964	3.336	0.022	0.001
		Validation	7.839	0.961	5.417	0.039	-0.007
		Test	7.777	0.935	6.195	0.037	-0.004
	ADA	Train	5.152	0.953	4.146	0.025	0.001
		Validation	8.479	0.947	6.377	0.043	-0.005
		Test	7.828	0.928	6.272	0.038	0.000
SVGA	Train	2.451	0.992	1.943	0.033	-0.005	
	Validation	3.849	0.982	2.764	0.053	0.006	
	Test	3.418	0.981	2.733	0.045	-0.003	
SVCB	Train	3.618	0.982	2.903	0.048	-0.013	
	Validation	4.714	0.972	3.271	0.065	0.002	
	Test	4.229	0.971	3.193	0.056	-0.008	
SVR	Train	4.451	0.972	3.584	0.060	-0.008	
	Validation	5.097	0.970	4.198	0.071	-0.009	
	Test	5.262	0.958	4.002	0.070	0.002	

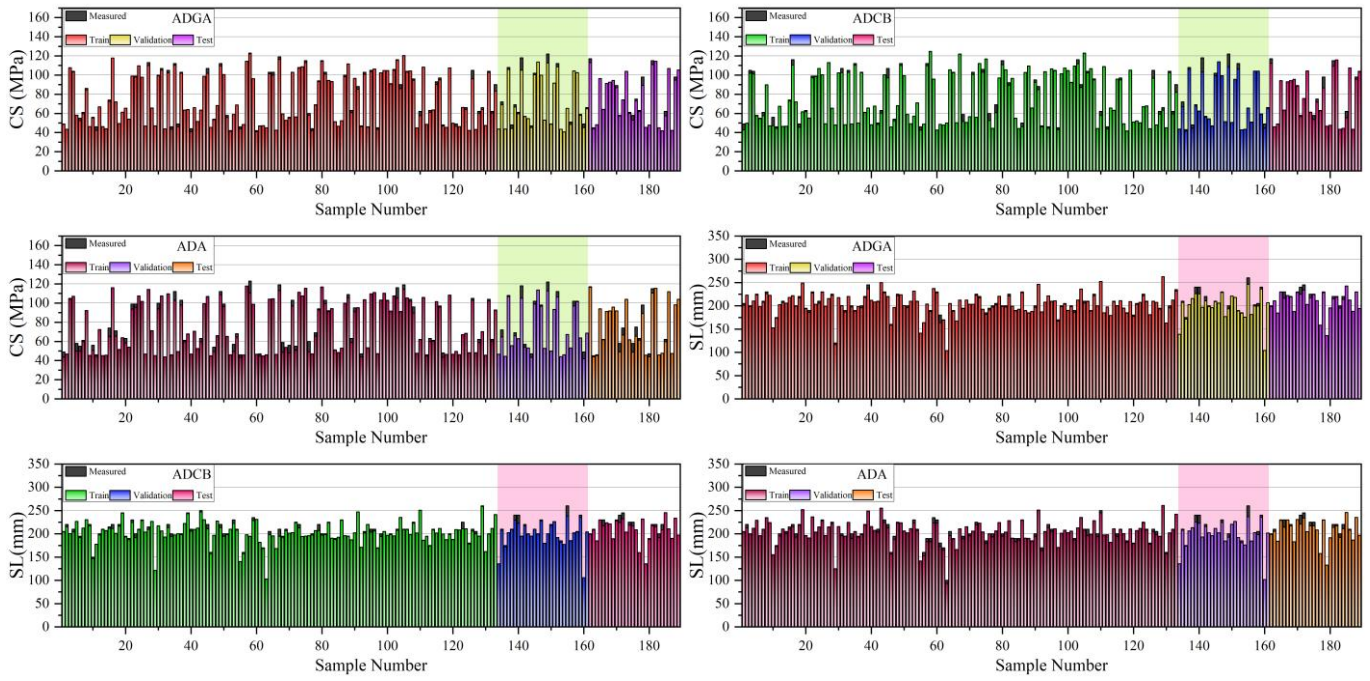


Fig. 4 The correlation of anticipated and measured values for CS and SL

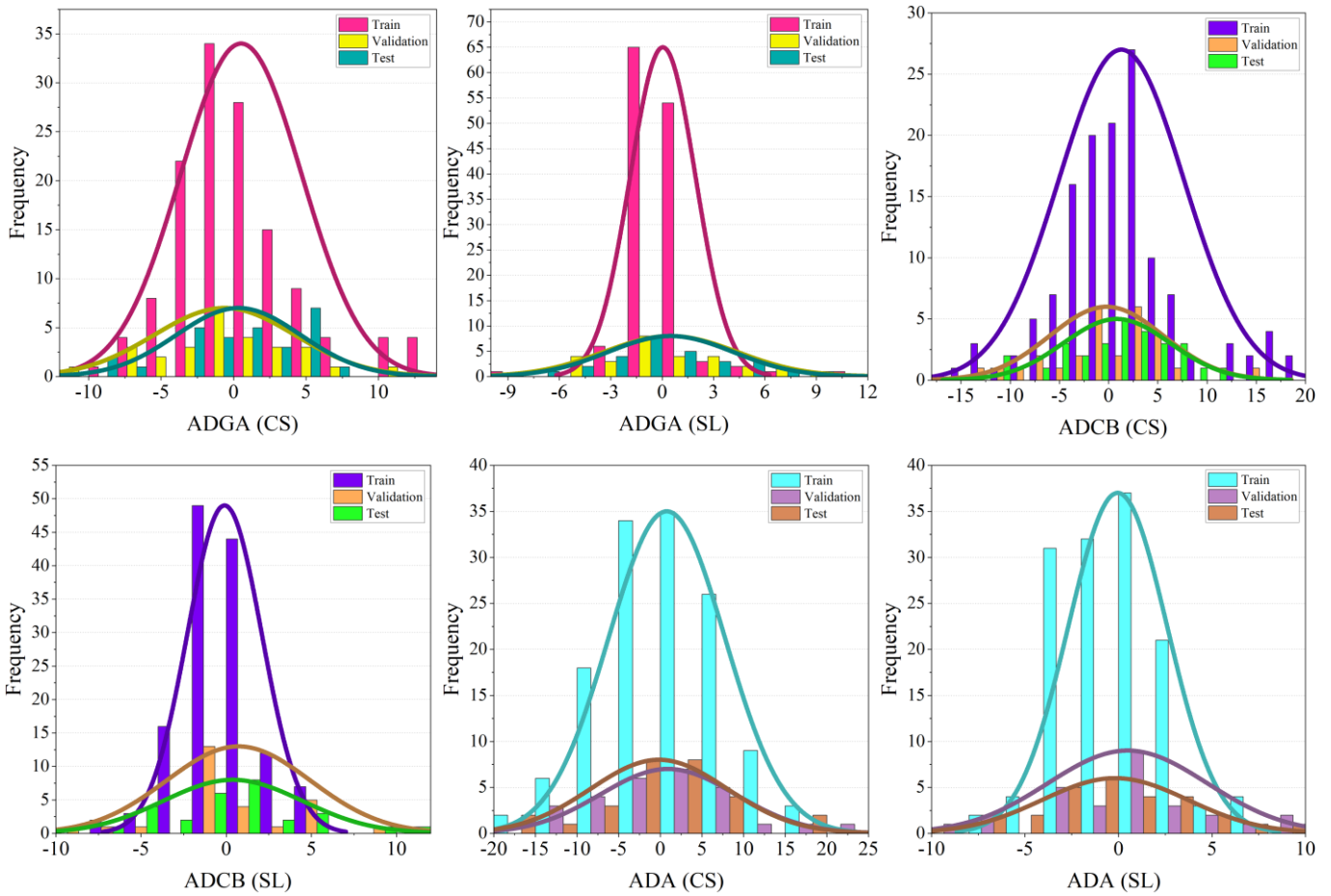


Fig. 5 The histogram distribution for the error percentage of the developed models

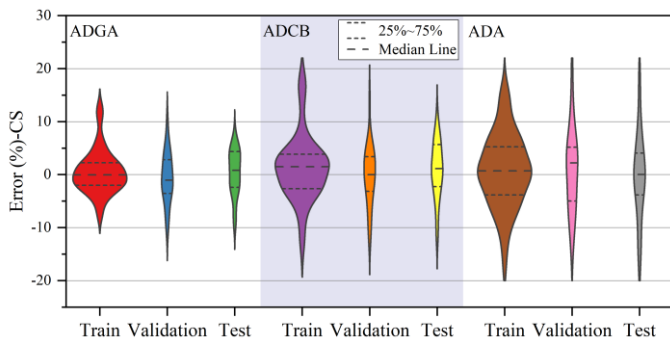


Fig. 6 The violin symbol plot for the errors of proposed frameworks

3.3 Attributes Analysis

SHAP (Shapley Additive Explanations) is a method used to interpret machine learning models by assigning each feature an important value based on its contribution to the model's predictions. It is rooted in cooperative game theory, providing fair and consistent feature importance, allowing for transparent and interpretable model results.

Fig. 7 presents the results of the SHAP analysis, which offers a deeper understanding of the impact of each input variable on the model's output. SHAP values allow us to assess the contribution of each feature to predictions, providing transparency and interpretability in machine learning models. In the case of CS, the W/B and SP have the most significant influence, reflecting their key roles in enhancing the strength of high-performance concrete. The W/B controls the hydration process, affecting concrete's density and strength, while SP improves workability and compaction, indirectly influencing the concrete's strength. On the other hand, the AE shows minimal impact on the CS predictions, suggesting that its effect on strength is relatively smaller compared to the other factors. For SL, the analysis reveals that SP and W are the most influential variables, which aligns with their known role in regulating the flowability and consistency of concrete mixtures. SP helps reduce the viscosity of the mix, improving workability without compromising the strength, while W directly affects the concrete's consistency and ease of placement. Interestingly, the W/B has the lowest impact on slump, indicating that, while it affects both CS and SL, its effect on slump is less pronounced than the other variables. These findings underscore the importance of specific input parameters in determining the performance of high-performance concrete, with each variable contributing differently to the outcome. The SHAP analysis helps identify the dominant factors but also assists in making data-driven decisions to optimize mix design for improved performance in both CS and SL.

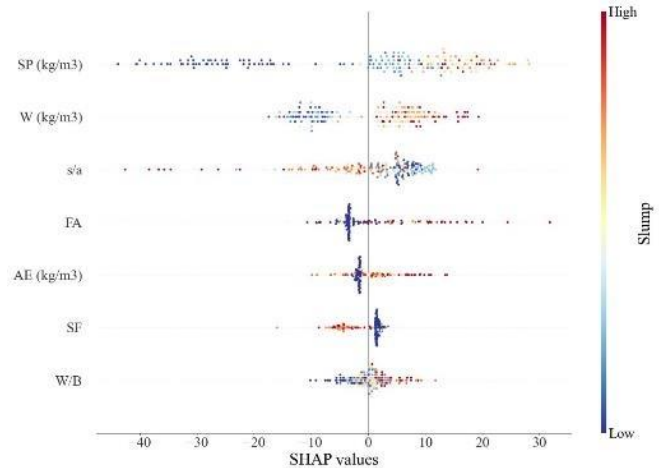
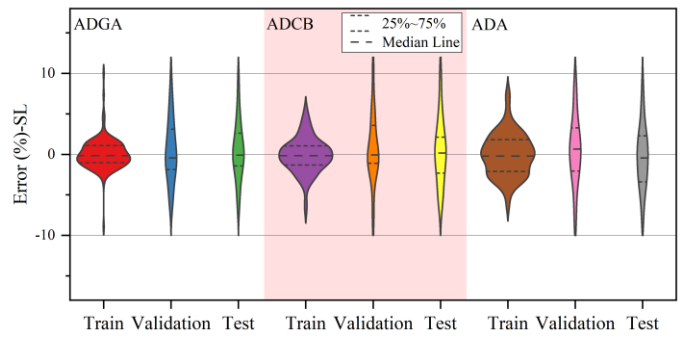
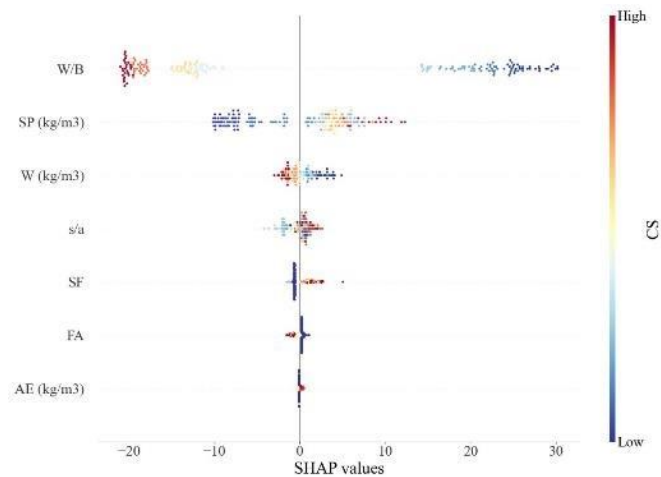


Fig. 7 The SHAP sensitivity analysis for the impact of the input variables on the model's output.

3.4 Practical implications of the study

The results of this study highlight the effectiveness of hybrid machine learning frameworks in accurately predicting CS and SL in HPC. These findings have significant practical implications for the construction industry, particularly in large-scale infrastructure projects where both mechanical performance and workability must be optimized.

1. **Enhanced Structural Performance and Safety**
The ADA+GOA (ADGA) model, achieving an R^2 of 0.992 with the lowest RMSE of 2.451, offers a precise predictive tool for estimating CS. This level of accuracy ensures that concrete mixtures meet the required load-bearing capacity, reducing risks associated with structural failure in critical applications such as bridges, high-rise buildings, and nuclear facilities. The ability to accurately predict CS before actual casting minimizes the likelihood of material wastage due to insufficient strength, thereby enhancing the reliability and safety of HPC structures over their service life.
2. **Optimized Workability and Construction Efficiency**
SL influences the ease of placement and consolidation, and optimizing its prediction ensures better control over concrete pouring and compaction processes, reducing inconsistencies during construction. By employing hybrid ML models, engineers can fine-tune mix proportions to balance workability with strength, reducing the need for excessive on-site adjustments, which can lead to cost overruns and project delays.
3. **Cost-Effective and Sustainable Mix Design**
The ability of ML models to predict HPC properties with high precision enables construction professionals to design concrete mixes efficiently, minimizing material overuse and optimizing the use of cement, aggregates, and additives. This optimization leads to lower carbon emissions in concrete production, aligning with sustainable construction initiatives. The ADGA model's superior accuracy ensures that engineers can reduce overdesign margins, thus promoting material efficiency and lowering costs without compromising durability.
4. **Limitations of SVR-Based Models and Future Considerations**
The poorer performance of SVR and its hybrid variants suggests that support vector regression may not be ideal for CS prediction, possibly due to nonlinear complexities in the dataset that require more adaptable frameworks like adaptive boosting (ADAR). Future research could explore incorporating additional hybrid optimizers or deep learning approaches to refine predictions further and extend applicability to various environmental conditions and material compositions.



4. Conclusions

The objective of this study is to estimate the compressive strength (CS) and slump (SL) of HPC using sophisticated ML regression frameworks, namely Adaptive Boosting Regression (ADAR) and Support Vector Regression (SVR), and employing two optimizers, namely Giant Armadillo Optimization Framework (GOA) and Chef Based Optimization Framework (CBOA). To enhance model outcomes, a decision was made to combine the frameworks with optimizers, creating new hybrid frameworks with increased precision and functionality. The results indicate that during the training step, the ADGA model exhibits the best operation in the CS target with an RMSE of 2.451 and an R2 value of 0.992. Subsequently, the ADCB model demonstrates improved functionality compared to the base model ADA, with an RMSE of 3.618 and an R2 value of 0.982. It is noteworthy that the operation of the SVR model and its hybrid forms is inferior to the ADA model in the CS target. While demonstrating the effectiveness of hybrid ML frameworks in predicting CS and SL in HPC, this study has certain limitations. One key limitation is dataset representativeness, as the data primarily comes from controlled experimental studies and published literature, which may not fully capture real-world variations in material properties, environmental conditions, and regional differences. A diverse dataset was used to mitigate this, and rigorous preprocessing techniques were applied to remove inconsistencies. However, future studies should incorporate larger and more regionally varied datasets to enhance model generalizability. Model selection bias is another factor, as the study primarily focused on ADAR and SVR combined with optimization algorithms (GOA and CBOA). While these models were chosen based on their strong regression capabilities, alternative ML techniques could be explored in future research. Additionally, computational cost is a consideration, as hybrid ML models with optimization algorithms require higher processing power, which may limit real-time implementation. Future work should focus on improving computational efficiency through feature selection techniques and lightweight model architectures. Lastly, while the study relied on existing experimental datasets for validation, direct experimental verification of predicted CS and SL values was not conducted. Future research should integrate laboratory testing to validate model predictions and assess discrepancies in theoretical and actual results. By addressing these limitations through careful dataset selection, model validation, and comparative analysis, this study enhances the reliability of its findings. Future extensions should focus on expanding datasets, testing additional ML models, and validating predictions experimentally to strengthen the practical applicability of ML-driven HPC mix design optimization.

References

- Abdullahi, M., 2012. Effect of aggregate type on compressive strength of concrete. *International journal of civil & structural engineering* 2, 791–800.
- Abuodeh, O.R., Abdalla, J.A., Hawileh, R.A., 2020. Assessment of compressive strength of Ultra-High-Performance Concrete using deep machine learning techniques. *Appl Soft Comput* 95, 106552.
- Aginam, C.H., Chidolue, C.A., Nwakire, C., 2013a. Investigating the effects of coarse aggregate types on the compressive strength of concrete. *Int J Eng Res Appl* 3, 1140–1144.
- Aginam, C.H., Umenwaliri, S.N., Nwakire, C., 2013b. Influence of mix design methods on the compressive strength of concrete. *ARNP Journal of Engineering and Applied Sciences* 8, 438–444.
- Ahmad, A., Farooq, F., Niewiadomski, P., Ostrowski, K., Akbar, A., Aslam, F., Alyousef, R., 2021a. Prediction of compressive strength of fly ash-based concrete using individual and ensemble algorithm. *Materials* 14, 794.
- Ahmad, A., Farooq, F., Ostrowski, K.A., Śliwa-Wieczorek, K., Czarnecki, S., 2021b. Application of novel machine learning techniques for predicting the surface chloride concentration in concrete containing waste material. *Materials* 14, 2297.
- Ahmad, A., Ostrowski, K.A., Maślak, M., Farooq, F., Mehmood, I., Nafees, A., 2021c. Comparative study of supervised machine learning algorithms for predicting the compressive strength of concrete at high temperature. *Materials* 14, 4222.
- Ahmad, W., Ahmad, A., Ostrowski, K.A., Aslam, F., Joyklad, P., Zajdel, P., 2021. Application of advanced machine learning approaches to predict the compressive strength of concrete containing supplementary cementitious materials. *Materials* 14, 5762.
- Alexandridis, A., Stavarakas, I., Stergiopoulos, C., Hloupis, G., Ninos, K., Triantis, D., 2015. Non-destructive assessment of the three-point-bending strength of mortar beams using radial basis function neural networks. *Computers and Concrete* 16, 919–932.
- Algaifi, H.A., Alqarni, A.S., Alyousef, R., Bakar, S.A., Ibrahim, M.H.W., Shahidan, S., Ibrahim, M., Salami, B.A., 2021. Mathematical prediction of the compressive strength of bacterial concrete using gene expression programming. *Ain Shams Engineering Journal* 12, 3629–3639.
- Ambroziak, A., Ziolkowski, P., 2020. Concrete compressive strength under changing environmental conditions during placement processes. *Materials* 13, 4577.
- Amin, M.N., Iqtidar, A., Khan, K., Javed, M.F., Shalabi, F.I., Qadir, M.G., 2021. Comparison of Machine Learning Approaches with Traditional Methods for Predicting the Compressive Strength of Rice Husk Ash Concrete. *Crystals* (Basel) 11, 779. <https://doi.org/10.3390/cryst11070779>
- Atiş, C.D., Özcan, F., Kılıç, A., Karahan, O., Bilim, C., Severcan, M.H., 2005. Influence of dry and wet curing conditions on compressive strength of silica fume concrete. *Build Environ* 40, 1678–1683.
- Chaabene, W. Ben, Flah, M., Nehdi, M.L., 2020. Machine learning prediction of mechanical properties of concrete: Critical review. *Constr Build Mater* 260, 119889.
- Chen, L., Kou, C.-H., Ma, S.-W., 2014. Prediction of slump flow of high-performance concrete via parallel hyper-cubic gene-expression programming. *Eng Appl Artif Intell* 34, 66–74. <https://doi.org/10.1016/j.engappai.2014.05.005>
- DeRousseau, M.A., Kasprzyk, J.R., Srubar, W. V., 2018. Computational design optimization of concrete mixtures: A review. *Cem Concr Res* 109, 42–53. <https://doi.org/10.1016/j.cemconres.2018.04.007>
- Dushimimana, A., Niyonsenga, A.A., Nzamurambaho, F., 2021. A review on strength development of high-performance concrete. *Constr Build Mater* 307, 124865.
- Farzadnia, N., Ali, A.A.A., Demirboga, R., 2011. Incorporation of mineral admixtures in sustainable high-performance concrete. *International Journal of Sustainable Construction Engineering and Technology* 2.
- Hasan, N.M.S., Sobuz, M.H.R., Khan, M.M.H., Mim, N.J., Meraz, M.M., Datta, S.D., Rana, M.J., Saha, A., Akid, A.S.M., Mehedi, M.T., 2022. Integration of rice husk ash as supplementary cementitious material in the production of sustainable high-strength concrete. *Materials* 15, 8171.
- Islam, M.N., Mohd Zain, M.F., Jamil, M., 2012. Prediction of strength and slump of rice husk ash incorporated high-performance concrete. *Journal of civil engineering and management* 18, 310–317. <https://doi.org/doi.org/10.3846/13923730.2012.698890>
- Jonnalagadda, S., Chava, S., 2023. Ultra-High-Performance Concrete (UHPC): A state-of-the-art review of material behavior, structural applications and future. *Electronic Journal of Structural Engineering* 23, 25–30.
- Khajavi, E., Taghavi Khanghah, A.R., Javadzade Khiavi, A., 2025. An efficient prediction of punching shear strength in reinforced concrete slabs through boosting methods and metaheuristic algorithms. *Structures* 74, 108519. <https://doi.org/https://doi.org/10.1016/j.istruc.2025.108519>
- Kim, J.-K., Yi, S.-T., 2002. Application of size effects to compressive strength of concrete members. *Sadhana* 27, 467–484.
- Liu, F., Li, Q.M., 2019. Strain-rate effect on the compressive strength of brittle materials and its implementation into material strength model. *Int J Impact Eng* 130, 113–123.
- Mahajan, L., Mahadik, S., Bhagat, S.R., 2020. Investigation of fly ash concrete by slump cone and compaction factor test, in: *IOP Conference Series: Materials Science and Engineering*. IOP Publishing, p. 12011.
- Malhotra, H.L., 1956. The effect of temperature on the compressive strength of concrete. *Magazine of concrete research* 8, 85–94.
- Moccia, F., Yu, Q., Fernández Ruiz, M., Muttoni, A., 2021. Concrete compressive strength: From material characterization to structural value. *Structural Concrete* 22, E634–E654.
- Mosaberpanah, M.A., Umar, S.A., 2020. Utilizing rice husk ash as supplement to cementitious materials on performance of ultra high-performance concrete: –a review. *Materials Today Sustainability* 7, 100030.
- Murali, G., Haridharan, M.K., Abid, S.R., Mohan, C., Khera, G.S., Bandhavi, C., 2023. Compressive strength and impact strength of preplaced aggregate fibre reinforced concrete. *Mater Today Proc*.
- Naeim, B., Akbarzadeh, M.R., Jahangiri, V., 2024a. Machine learning-based prediction of seismic response of elevated steel tanks. *Structures* 70, 107649. <https://doi.org/https://doi.org/10.1016/j.istruc.2024.107649>
- Naeim, B., Khiavi, A.J., Dolatimehr, P., Sadaghat, B., 2024b. Novel Optimized Support Vector Regression Networks for Estimating Fresh and Hardened Characteristics of SCC.
- Napoli, A., Realfonzo, R., 2020. Compressive strength of concrete confined with fabric reinforced cementitious matrix (FRCM): Analytical models. *Composites Part C: Open Access* 2, 100032.
- Ngugi, H.N., Mutuku, R.N., Gariy, Z.A., 2014. Effects of sand quality on compressive strength of concrete: A case of Nairobi County and Its Environs, Kenya. *Open Journal of Civil Engineering* 2014.

Ni, H.-G., Wang, J.-Z., 2000. Prediction of compressive strength of concrete by neural networks. *Cem Concr Res* 30, 1245–1250.

Obi Lawrence, E., 2016. Empirical investigation of the effects of water quality on concrete compressive strength. *international journal of constructive research in civil engineering* 2, 30–35.

Parande, A.K., 2013. Role of ingredients for high strength and high-performance concrete—a review. *Advances in concrete construction* 1, 151.

Paudel, S., Pudasaini, A., Shrestha, R.K., Kharel, E., 2023. Compressive strength of concrete material using machine learning techniques. *Clean Eng Technol* 15, 100661.

Pourbaba, M., Asefi, E., Sadaghian, H., Mirmiran, A., 2018. Effect of age on the compressive strength of ultra-high-performance fiber-reinforced concrete. *Constr Build Mater* 175, 402–410.

Ruggieri, S., Cardellicchio, A., Leggieri, V., Uva, G., 2021. Machine-learning based vulnerability analysis of existing buildings. *Autom Constr* 132, 103936.

Sadaghat, B., Ebrahimi, S.A., Souri, O., Yahyavi Niar, M., Akbarzadeh, M.R., 2024. Evaluating strength properties of Eco-friendly Seashell-Containing Concrete: Comparative analysis of hybrid and ensemble boosting methods based on environmental effects of seashell usage. *Eng Appl Artif Intell* 133, 108388. <https://doi.org/10.1016/j.engappai.2024.108388>

Salem, M.A.A., Pandey, R.K., 2015. Effect of cement-water ratio on compressive strength and density of concrete. *International Journal of Engineering Research and Technology (IJERT)* 4.

Shah, H.A., Rehman, S.K.U., Javed, M.F., Iftikhar, Y., 2022. Prediction of compressive and splitting tensile strength of concrete with fly ash by using gene expression programming. *Structural Concrete* 23, 2435–2449. <https://doi.org/10.1002/suco.202100213>

Sharma, R., 2021. Effect of wastes and admixtures on compressive strength of concrete. *Journal of Engineering, Design and Technology* 19, 219–244.

Silveira, L., de Almeida Jácomo, A.T., Furtado, M.M., Torres, N.M., Sollmann, R., Vynne, C., 2009. Ecology of the giant armadillo (*Priodontes maximus*) in the grasslands of central Brazil. *Edentata* 2009, 25–34.

Song, H., Ahmad, A., Farooq, F., Ostrowski, K.A., Maślak, M., Czarnecki, S., Aslam, F., 2021a. Predicting the compressive strength of concrete with fly ash admixture using machine learning algorithms. *Constr Build Mater* 308, 125021.

Song, H., Ahmad, A., Ostrowski, K.A., Dudek, M., 2021b. Analyzing the compressive strength of ceramic waste-based concrete using experiment and artificial neural network (ANN) approach. *Materials* 14, 4518.

Sun, J., Ma, Y., Li, J., Zhang, J., Ren, Z., Wang, X., 2021. Machine learning-aided design and prediction of cementitious composites containing graphite and slag powder. *Journal of Building Engineering* 43, 102544.

Tan, Z., Bernal, S.A., Provis, J.L., 2017. Reproducible mini-slump test procedure for measuring the yield stress of cementitious pastes. *Mater Struct* 50, 1–12.

Tasevski, D., Fernández Ruiz, M., Muttoni, A., 2019. Assessing the compressive strength of concrete under sustained actions: From refined models to simple design expressions. *Structural Concrete* 20, 971–985.

Tavana Amlashi, A., Mohammadi Golafshani, E., Ebrahimi, S.A., Behnood, A., 2023. Estimation of the compressive strength of green concretes containing rice husk ash: a comparison of different machine learning approaches. *European Journal of Environmental and Civil Engineering* 27, 961–983. <https://doi.org/10.1080/19648189.2022.2068657>

Trojovská, E., Dehghani, M., 2022. A new human-based metaheuristic optimization method based on mimicking cooking training. *Sci Rep* 12, 14861.

Vu, C.-C., Plé, O., Weiss, J., Amitrano, D., 2020. Revisiting the concept of characteristic compressive strength of concrete. *Constr Build Mater* 263, 120126.

Yen, T., Tang, C.-W., Chang, C.-S., Chen, K.-H., 1999. Flow behaviour of high strength high-performance concrete. *Cem Concr Compos* 21, 413–424.

Zhutovsky, S., Kovler, K., 2017. Influence of water to cement ratio on the efficiency of internal curing of high-performance concrete. *Constr Build Mater* 144, 311–316.

Disclaimer

The statements, opinions and data contained in all publications are solely those of the individual author(s) and contributor(s) and not of EJSEI and/or the editor(s). EJSEI and/or the editor(s) disclaim responsibility for any injury to people or property resulting from any ideas, methods, instructions or products referred to in the content.